Investigation of Evolution in the Synthesis of Graphene Oxide and Reduced Graphene Oxide

Anwar, Hafeez*[*+]; Bin Amin, Ahmad; Iqbal, Mujahid; Haseeb, Muhammad; Hanif, Sabiha; Khalid, Maryam; Sajid, Huma; Abbas, Beenish

Department of Physics, University of Agriculture, Faisalabad, PAKISTAN

Ul Hassan, Mahmoud

Pakistan Nuclear Regulatory Authority (PNRA), Islamabad, PAKISTAN

Dissanayake, M. A. K. L.

National Institute of Fundamental Studies, SRI LANKA

ABSTRACT: *Hummer's method, in which potassium permanganate ($KMnO_4$) acts as the oxidant and concentrated sulfuric acid (H_2SO_4) serves as the intercalator is commonly used to prepare Graphene Oxide (GO). The amount of the intercalator, oxidant, and graphite are important factors that affect the properties and structure of graphene oxide. In this work, a detailed investigation is carried out to optimize the mechanism of Hummer's method in order to get the maximum yield of GO and reduced graphene oxide (rGO). XRD, SEM, TEM, FT-IR, TGA, Raman spectroscopy, and UV-Visible spectroscopy are used for characterization. XRD results of optimized samples (Opt-3-GO and Opt-3-rGO) clearly showed that the value of interlayer spacing is increased due to increasing the amount of oxidant and intercalator. SEM and TEM results revealed that the Opt-3-rGO was highly wrinkled nanosheets as compared to the Opt-3-GO. The FT-IR results showed that the double amount of oxidant and intercalator had an effect on the functional groups in the structure of Opt-3-GO and Opt-3-rGO. TGA results indicated that Opt-3-rGO has higher thermal stability as compared to Opt-3-GO due to the lower defect density. The ratio of intensities of D and G bands (I_D/I_G) increased for Opt-3-rGO as compared to Opt-3-GO. UV-Vis spectra of Opt-3-GO showed a maximum absorption peak at 237 nm attributable to π-π* transition of the atomic C-C bonds. The prepared samples have their use in different applications such as electrode materials for batteries, capacitors, and solar cells.*

KEYWORDS: *Graphene Oxide (GO), Reduced graphene oxide (rGO), Improved Hummer's method, Oxidant, Intercalator.*

INTRODUCTION

In order to synthesize Graphene Oxide (GO), Hummer's method is generally used [1]. There are three steps that are involved in the formation of GO from bulk graphite [2]. Firstly, sulfuric acid (H_2SO_4) is used as

* *To whom correspondence should be addressed.*
+ *E-mail: hafeez.anwar@gmail.com*
1021-9986/2022/12/3905-3912 8/$/5.08

the intercalation agent for graphite which is converted into the Graphite Intercalation Compound (GIC) [3]. This GIC is a critical intermediate because it allows oxidizing agents to diffuse in the interlayer spaces of graphite. Secondly, the graphite intercalation compound is converted into pristine oxidized graphite. This process is used to control the diffusion. Thirdly, pristine oxidized graphite is converted into GO. Hence, during the preparation of GO, intercalation of graphite requires subsequent exfoliation. In the traditional Hummer method, potassium permanganate ($KMnO_4$) is used as the main oxidant with some auxiliary agents such as sodium nitrate ($NaNO_3$). The stoichiometry of the chemicals and synthesis process has effect on the properties of GO [4]. Many researchers have investigated this and introduced improvements in Hummer's method by surmount these short comings. In previous works, the improvements of the Hummer's method suggested to avoid the use of $NaNO_3$. Replacement of $NaNO_3$ was compensated by increasing the amount of $KMnO_4$ for the improvement [5-9]. Many researchers used $NaNO_3$ in the preparation of GO, in which the amount of $NaNO_3$ was varied. Whereas, the same amount of graphite was used [10]. *Sherif* [11] reported that $NaNO_3$ acted as an oxidant in the preparation mechanism of GO. In another study, $NaNO_3$ was not used which suggested its negligible role in the oxidation of graphite [12]. *Chen* reported $NaNO_3$ assisted H_2SO_4 intercalation, which is very helpful to the oxidation of graphite by the oxidant [13]. For the graphite prior to the formation of GO, *Wu* [14] reported that $NaNO_3$ acts as an agent of intercalation. Mombeshora [15] studied the physicochemical properties of GO and also investigated the effects on oxygen content due to the different ratios of graphite/$NaNO_3$. It can be deduced from this discussion that the mechanism and role of $NaNO_3$ still need to be investigated to further make this process efficient. Flake graphite is commonly used for the preparation of GO. The structure of flake graphite contains some defects that can act as reaction sites for oxidation [16-18]. *Seyyedeh et al*., reported that under identical conditions, a small size of graphite was considered as a time saver as compared to the larger size of graphite due to their lower resistance [19].

The sheets of the rGO are considered as chemically derived graphene. There are many methods for the synthesis of rGO such as chemical reduction of GO, electrochemical production of rGO, and thermal reduction [20]. For mass production, there are two methods that are very impressive such as electrochemical and chemical reduction of GO [21]. The excellent properties of GO and rGO make these very useful materials for many applications and are thus widely investigated by researchers [22-25].

In this work, a detailed investigation is carried out to understand the mechanism lying behind the growth of GO from graphite by performing a series of experiments. The factors affecting the preparation of GO were systematically studied *via* XRD, SEM, TEM, FT-IR, TGA, Raman spectroscopy and UV–Visible spectroscopy. Therefore, the outcomes of this study are critical and helpful in order to get optimized oxidation of graphite thus having a maximum yield of GO. After the optimization of GO, rGO was also prepared.

EXPERIMENTAL SECTION

Chemical and reagents

All the chemicals and reagents used were of analytical grade and were purchased from sigma- Aldrich. Graphite powder (particle size + 100 mesh), Sulfuric acid (H_2SO_4, 98%), Sodium Nitrate ($NaNO_3$), Potassium permanganate ($KMnO_4$), Graphene oxide (GO), Hydrochloric acid (HCl), Sodium borohydride ($NaBH_4$), Hydrogen peroxide (H_2O_2) and Sodium hydroxide (NaOH) were used without further purification in this work.

Synthesis of Graphene Oxide (GO)

Conventional Hummer's method was used to prepare graphene oxide. Graphite powder (1.5 g) was mixed with 70 ml of concentrated H_2SO_4 (98 %) under constant stirring. When the graphite powder was dissolved then suitable stoichiometric amount of $NaNO_3$ was added in the solution and continuous stirring was done. After this, $KMnO_4$ was slowly added in the above solution and further stirred for 1 h. It was an exothermic process and large amount of heat produced so that beaker was placed in the ice-bath to lower the reaction temperature (~10 ºC). Further, the solution was stirred at 65 ºC for 1 h. After this, 300 ml of DI water was poured into the solution and stirred for 3 h. In order to stop the process of oxidation, H_2O_2 and HCl were added to separate the layers of graphite oxide. The solution was washed many times with de-ionized water in order to maintain pH at 7 and was collected by centrifugation. The sample was dried in an oven (Model Shel-Lab) at 80 ºC and thus GO was obtained as shown in Fig. 1(a). In order get to full oxidation of graphite to GO and to get maximum yield, a series of experiments were conducted.

Table. 1: Detail of experiments having different amounts of precursors.

Sample	Graphite powder (g)	$KMnO_4$ (g)	H_2SO_4 (ml)	$NaNO_3$ (g)
Opt-1-GO	1.5	6	60	1
Opt-2-GO	1.5	7	70	1
Opt-3-GO	1.5	8	80	1
Opt-4-GO	1.5	9	90	1
Opt-5-GO	1.5	10	100	1

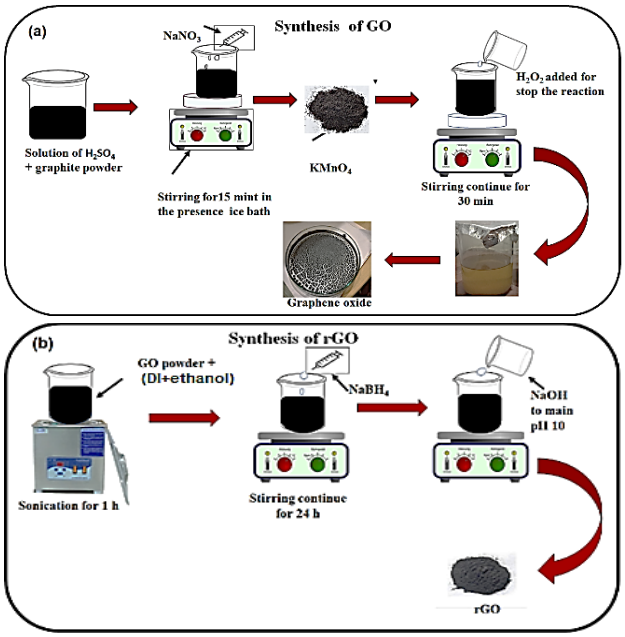

Fig. 1: Schematic diagram for the synthesis of (a) Opt-3-GO and (b) Opt-3-rGO.

Regarding this, experiments were conducted with different amounts of $KMnO_4$, H_2SO_4 as shown in Table 1. The prepared samples were labeled as Opt-1-GO, Opt-2-GO, Opt-3-GO, Opt-4-GO and Opt-5-GO. The maximum yield of GO was obtained by sample Opt-3-GO.

Synthesis of Opt-3-rGO

Reduced graphene oxide was prepared by mixing the appropriate amount of Opt-3-GO powder in the (DI + ethanol) and sonicated for 1 h to make a good suspension as shown in Fig. 1b. Aqueous solution of Sodium borohydrite was prepared and added dropwise into prepared GO suspension with continuously stirring at room temperature for 24 h. Sodium borohydrite acted as a reducing agent. NaOH was used to maintain pH at 10. The solution was washed and dried in an oven (Model Shel-Lab) at 85 ºC to obtain Opt-3-rGO.

Characterization

The prepared samples were characterized using X-Ray Diffraction [Model (PANalytical)] with Nickel filtered CuK_α (λ = 1.50405 Å) radiation. Scherer's formula was used to calculate the average crystallite size. The surface morphology and structural features were characterized using the SEM Model (JEOL-JSM 5910) and Transmission Electron Microscopy (TEM) (Tecnai G F30 S-Twin made by FEI Company). Fourier Transform InfraRed (FT-IR) spectra of the samples were recorded on Nicolet Is50, in the range of 500-4000 cm^{-1}. ThermoGravimetric Analysis (TGA) was performed using TG209F3 apparatus at the heating rate of 10 ºC min^{-1} from 100 to 1000 ºC. Raman measurements were done by the FT-Raman made by Bruker, Germany. The absorption spectra of prepared samples were recorded with UV-Vis spectrophotometer PG Model T-80. The spectra were recorded in the range of (200-800 nm).

RESULTS AND DISCUSSION

X-ray diffraction analysis

XRD results of graphite, GO and rGO prepared for the conventional Hummers method are shown in Fig. 2a. Using the Bragg equation, the d-spacing of graphite, GO and rGO were calculated to be 0.3355, 0.3366, 0.3363 nm. X-ray patterns of graphite, Opt-3-GO, and Opt-3-rGO prepared by improved Hummer's method are only shown in Fig. 2b as the maximum yield of GO was obtained by Opt-3GO. The graphite showed a basal reflection (002) peak at $2\theta = 26.60^{\circ}$. The interlayer d-spacing of graphite, Opt-3-GO, and Opt-3-rGO is 0.7775, 0.8335, and 0.8337 nm, respectively. A typical broad peak near $2\theta = 11^{\circ}$ was observed due to the formation of the oxygen-containing groups that confirmed the formation of GO as shown in Fig. 2b. This shows that double the amount of $KMnO_4$ along with H_2SO_4 gives maximum yield whereas $NaNO_3$ shows minute effects in the interlayer spacing of GO.

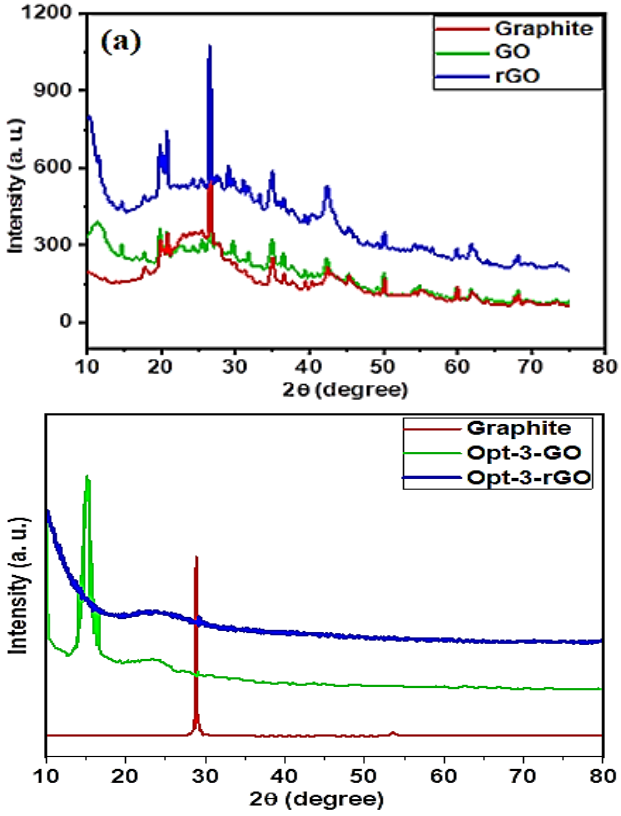

Fig. 2: X-ray diffraction patterns of graphite, (a) GO and rGO prepared by conventional Hummer's method, (b) Opt-3-GO and Opt-3-rGO prepared by improved Hummer's method.

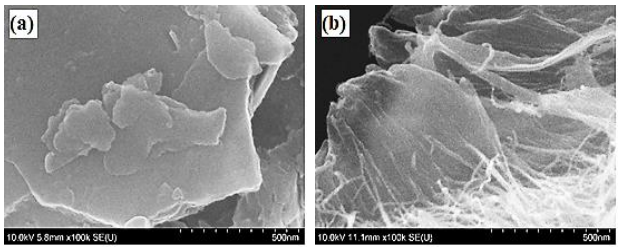

Fig. 3: Scanning electron micrographs of (a) Opt-3-GO (b)Opt-3-rGO.

Scanning electron microscopy and transmission electron microscopy analysis

The scanning electron micrographs of Opt-3-GO and Opt-3-rGO are shown in Fig. 3 (a, b). Opt-3-GO has 2-D sheet-like structure. Fig. 3(b) shows the highly wrinkled structure of Opt-3-rGO as compared to the Opt-3-GO. It was found that Opt-3-rGO has highly wrinkled nanosheets which are considered to have more sensitivity and show good recovery ability. While reduction of GO to rGO, the surface of the GO is conjugated due to the escape of oxygen from its surface [26-29].

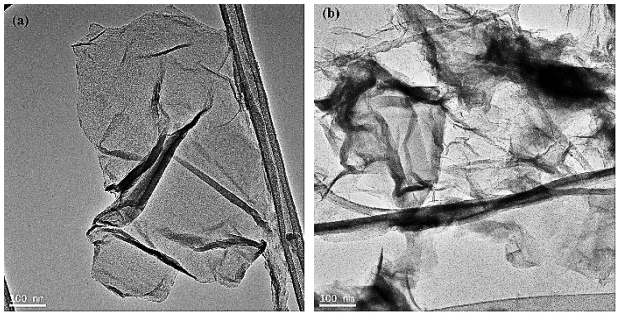

Fig. 4: TEM results of (a) Opt-3-GO (b) Opt-3-rGO.

TEM was used to investigate the microstructure of the Opt-3-GO and Opt-3-rGO. The TEM results of the Opt-3-GO show wrinkles and thick flattened nanosheets-like surface as shown in Fig. 4(a). It is due to the functional groups and electrostatics interaction of the oxides on the surface. Fig. 4(b) shows that Opt-3-rGO has 2D structure which is considered as the thermal by dynamic stable due to the ripple effects [30].

Fourier Transform InfraRed (FT-IR) spectroscopy analysis

FT-IR spectra of Opt-3-GO and Opt-3-rGO are shown in Fig. 5. The FT-IR spectrum of Opt-3-GO shows a broad peak between 3500 to 3300cm^{-1} due to the high frequency of the bending vibration and stretching of OH groups of water molecules adsorbed on Opt-3-GO. Thus, sample has strong hydrophilicity. For graphene oxide, the characteristic peaks for carboxyl C=O [31] were found at 1735cm^{-1}. By comparison of the FT-IR spectra of Opt-3-GO and Opt-3-rGO, it was evident that the peaks of the carboxyl showed lower intensity for the Opt-3-rGO and also oxygen functional groups were reduced after the reduction of Opt-3-GO. For both Opt-3-GO and Opt-3-rGO samples, aromatic C=C groups were seen at the peak of 1500 cm^{-1}. These oxygen groups revealed that graphite has been oxidized. In the case of Opt-3-rGO, a reduction in the intensity of the carboxyl C-O at 948 cm^{-1} and aromatic C=C at 1500 cm^{-1} was seen [32]. In this regard, the amount of oxidant and intercalator was increased and the results showed that the destroying structure of Opt-3-GO was increased by producing more carboxyl groups due to the edge selective oxidations.

Thermal Gravimetric Analysis (TGA)

The measurement of TGA was done in the temperature range of the 100 to 1000 ºC under nitrogen to study the

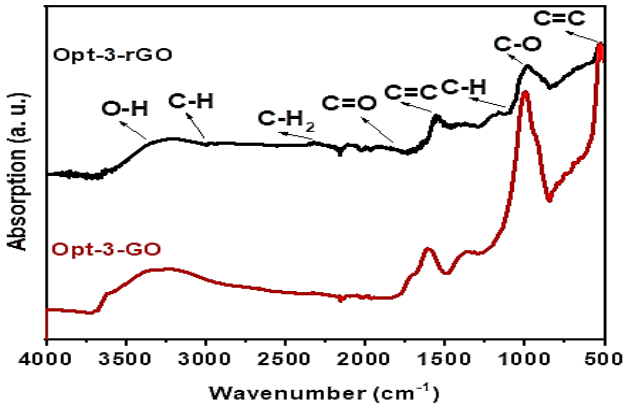

Fig. 5: FT-IR spectra of Opt-3-GO and Opt-3-rGO.

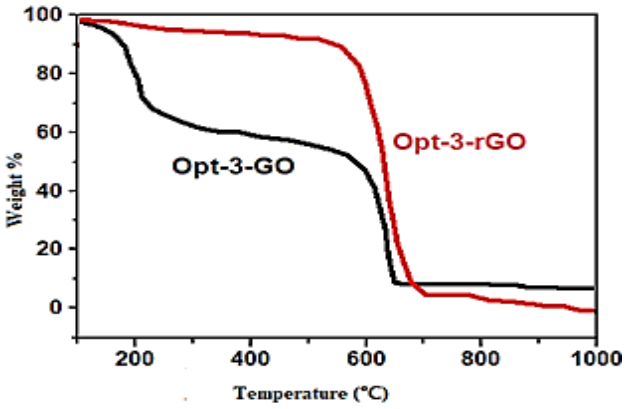

Fig. 6: TGA plots of Opt-3-GO and Opt-3-rGO.

thermal stability of Opt-3-GO and Opt-3-rGO and the obtained TGA plots are shown in the Fig. 6. In both samples, the significant mass was loosed. GO was decomposed in different steps, i.e, in the range of 200 to 500 ºC the first weight loss 30 % was taken. Within this range of temperature, the removal of water, carbon oxidation, and decomposition of oxygen groups was completed. Before 700 ºC it was clearly observed that the carbon is completely decomposed. Compared with Opt-3-GO, the Opt-3-rGO has better stability before 500 ºC and also completely decomposed at about 700 ºC. The stable state of the Opt-3-rGO is attributable to low defect density. Therefore, Opt-3-rGO shows relatively better stability till 730 ºC [33].

Raman spectroscopy analysis

For the study of structural information, Raman spectroscopy, a non-destructive technique, was used. In the Raman spectra, the graphitic carbon-based materials have G peaks, D peaks and their overtones. The intensity peaks of the G band at 1580 cm^{-1} and the 2D band at 2700 cm^{-1} were observed. Due to the G band, bond stretching of all the sp^2 atoms in the form of chains and rings occurred. The 2D band (G* band) is also observed in the graphite oxide. The peak at 1350cm^{-1} is known as the D peak. Due to the defects in the samples, the D peak shows an increase in the breathing mode of aromatic rings.

The Raman spectra of Opt-3-GO and Opt-3-rGO are shown in Fig.7. It is observed that there is a strong D peak at 1350 cm^{-1} as compared to the intensity of the G peak at 1580 cm^{-1}. The 2D peak is at about 2680 cm^{-1}. D+G is also known as defect activated peak which is observed at 2950 cm^{-1}.

The size of grain in the sp^2 region of Opt-3-GO and Opt-3-rGO were calculated by using the following equation.

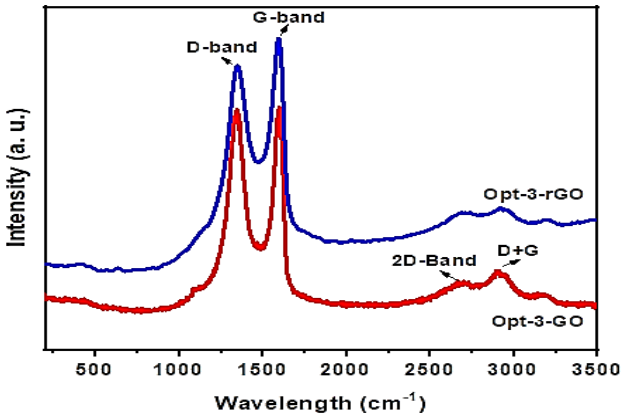

Fig. 7: Raman spectrum of Opt-3-GO and Opt-3-rGO.

$$La = \frac{[2.4 \times 10^{-10} (\lambda_i^4)]}{[\frac{I_D}{I_G}]} \quad (1)$$

Where La is the size of grain, I_G and I_D relative intensity of the G and D peaks, respectively, and λ_i is the laser wavelength which is 532 nm. The value of relative intensity ratio I_D/I_G of Opt-3-GO and Opt-3-rGO is found to be 0.80 and 0.84 respectively, and the corresponding average grain sizes were found to be 24.03 nm and 22.88 nm, respectively. The result shows that the effects of the H_2SO_4 and $NaNO_3$ improved the degree of oxidation in the graphite when a large amount of oxidant and intercalator were used. $NaNO_3$ is not conducive to the diffusion of oxidants and intercalators [34].

UV-Visible spectroscopy analysis

UV-Vis spectra of Opt-3-GO and Opt-3-rGO showed maximum strong absorption peaks at 237 nm and 240 nm respectively as shown in Fig. 8. This is attributed to the π-π* (212.6 nm) transition of the C-C bonds. In the process of

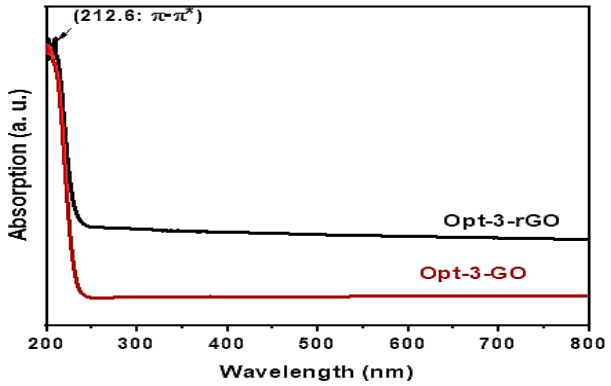

Fig. 8: UV-vis spectra of Opt-3-GO and Opt-3-rGO.

reduction, some of the oxygen group is removed in the Opt-3-rGO. Therefore, Opt-3-rGO showed semiconductor or semi-metal behavior [35].

CONCLUSIONS

We developed an improved Hummer method for the synthesis of GO. When the double amount of $KMnO_4$ and H_2SO_4 were used, the oxidation degree of graphite was found higher. To the diffusion of intercalator and oxidant, the $NaNO_3$ was not suggested as a conductive. The amount of intercalator and oxidant was increased to improve the degree of GO and hence facilitated the preparation of GO. XRD results have shown that crystallinity is increased from GO to rGO in optimized samples, due to the formation of sp^2 network in rGO. SEM and TEM micrographs show that the surface of Opt-3-rGO is highly sensitive and wavier than the surface of Opt-3-GO. The analysis of FT-IR and TGA confirmed that the oxygen-containing functional groups are removed from GO due to their reduction. In Raman spectra, D, G and 2D bands clearly confirmed the characteristic structure of GO and rGO. The outcomes of this study are critical and helpful in order to get optimized oxidation of graphite for maximum yield of GO.

Acknowledgments

H. Anwar is grateful to the Pakistan Science Foundation for funding under the project PSF-NSF/Eng/P-UAF (05).

Received: Nov. 20, 2021 ; Accepted: Apr. 25, 2022

References

[1] Alkhouzaam A., Qiblawey H., Khraisheh M., Atieh M., Al-Ghouti M., Synthesis of Graphene Oxides Particle of High Oxidation Degree Using a Modified Hummers Method, *J. Ceramics International*, **46(15):** 23997–24007 (2020).

[2] Benzait Z., Chen P., Trabzon L., Enhanced Synthesis Method of Graphene Oxide, *J. Nanoscale Adv*, **3(1):** 223–230 (2021).

[3] Abaszade R.G., Mamedova S.A., Agayev F.H., Budzulyak S.I., Kapush O.A., Mamedova M.A., Nabiyev A.M., Kotsyubynsky V.O., Synthesis and Characterization of Graphene Oxide Flakes for Transparent Thin Films, *J. Phys. Chem. Solid State*, **22(3):** 595–60 (2021).

[4] Hou Y., Lv S., Liu L., Liu X., High-Quality Preparation of Graphene Oxide via the Hummers' Method: Understanding the Roles of the Intercalator, Oxidant, and Graphite Particle Size, *J. Ceramics International*, **46(2):** 2392-2402 (2020).

[5] Nasreen F., Anwar A. W., Ahmad M. A., Majeed A., Afzal A., Hussain T., A Facile Improved Oxidation Method for Ecological Production of Graphene Oxide, *J. Dig. J. Nanomater. Biostructures*, **16(1):** 119–124 (2021).

[6] Alkhouzaam A., Qiblawey H., Khraisheh M., Atieh M., Al-Ghouti M., Synthesis of Graphene Oxides Particle of High Oxidation Degree using a Modified Hummers Method, *J. Ceramics International*, **46(15):** 23997-24007 (2020).

[7] Manabe S., Kiliyankil S.A., Takiguchi S., Kumashiro T., Fugetsu B., Sakata I., Graphene Nanosheets Homogeneously Incorporated in Polyurethane Sponge for the Elimination of Water-Soluble Organic Dyes, *J. of Colloid and Interface Science*, **584:** 816-826 (2021).

[8] Lee K.E., Kim J.E., Maiti U.N., Lim J., Hwang J.O., Shim J., Kim S.O., Liquid Crystal Size Selection of Large-Size Graphene Oxide for Size-Dependent N-Doping and Oxygen Reduction Catalysis, *J. ACS Nano*, **8(9):** 9073-9080 (2014).

[9] Ma H., Li C., Zhang M., Hong J.D., Shi G., Graphene Oxide Induced Hydrothermal Carbonization of Egg Proteins for High-Performance Supercapacitors, *J. Materials Chemistry A*, **5(32):** 17040-17047 (2017).

[10] Chen J., Li Y., Huang L., Li C., Shi G., High-Yield Preparation of Graphene Oxide from Small Graphite Flakes via An Improved Hummers Method with a Simple Purification Process, *J. Carbon*, **81:** 826-834 (2015).

[11] El-Khodary S.A., El-Enany G.M., El-Okr M., Ibrahim M., Preparation and Characterization of Microwave Reduced Graphite Oxide for High-Performance Supercapacitors, *J. Electrochimica Acta*, **150:** 269-278 (2014).

[12] Quitain A.T., Sumigawa Y., Mission E.G., Sasaki M., Assabumrungrat S., Kida T., Graphene Oxide and Microwave Synergism for Efficient Esterification of Fatty Acids, *J. Energy & Fuels*, **32(3):** 3599-3607 (2018).

[13] Chen J., Yao B., Li C., Shi G., An Improved Hummers Method for Eco-Friendly Synthesis of Graphene Oxide, *J. Carbon*, **64:** 225-229 (2013).

[14] Wu T.T., Ting J.M., Preparation and Characteristics of Graphene Oxide and its Thin Films, *J. surface and coatings technology*, **231:** 487-491 (2013).

[15] Mombeshora E.T., Ndungu P.G., Nyamori V.O., Effect of Graphite/Sodium Nitrate Ratio and Reaction Time on the Physicochemical Properties of Graphene Oxide, *J. New Carbon Materials*, **32(2):** 174-187 (2017).

[16] Holm A., Park J., Goodman E.D., Zhang J., Sinclair R., Cargnello M., Frank C.W., Synthesis, Characterization, and Light-Induced Spatial Charge Separation in Janus Graphene Oxide, *J. Chem. of Materials*, **30(6):** 2084-2092 (2018).

[17] Marcano D.C., Kosynkin D.V., Berlin J.M., Sinitskii A., Sun Z., Slesarev A., Tour J.M., Improved Synthesis of Graphene Oxide, *J. ACS Nano*, **4(8):** 4806-4814 (2010).

[18] Chen Z, Liu Y., Luo J., Tribological Properties of Few-Layer Graphene Oxide Sheets as Oil-Based Lubricant Additives, *Chinese J. Mechanical Engineering*, **29(2):** 439-444 (2016).

[19] Shojaeenezhad S.S., Farbod M., Kazeminezhad I., Effects of Initial Graphite Particle Size and Shape on Oxidation Time in Graphene Oxide Prepared by Hummers' Method, *J. Sci. Adv. Materials and Devices*, **2(4):** 470-475 (2017).

[20] Dimiev A.M., Bachilo S.M, Saito R., Tour J.M., Reversible Formation of Ammonium Persulfate/Sulfuric Acid Graphite Intercalation Compounds and Their Peculiar Raman Spectra, *J. ACS Nano*, **6(9):** 7842-7849 (2012).

[21] Liou Y.J., Tsai B.D., Huang W.J, An Economic Route to Mass Production of Graphene Oxide Solution for Preparing Graphene Oxide Papers, *J. Materials Science and Engineering: B*, **193:** 37-40 (2015).

[22] Cao J., Wang Y., Xiao P., Chen Y., Zhou Y., Ouyang J.H., Jia D, Hollow Graphene Spheres Self-Assembled from Graphene Oxide Sheets by a One-Step Hydrothermal Process, *J. Carbon*, **56:** 389-391 (2013).

[23] Guo P., Song H., Chen X, Hollow Graphene Oxide Spheres Self-Assembled by W/O Emulsion, *J. Materials Chemistry*, **20(23):** 4867-4874 (2010).

[24] Sharifzadeh E., Parsnasab M, Direct and Reverse Desymmetrization Process in O/W Pickering Emulsions to Produce Hollow Graphene Oxide Janus Micro/Nano-Particles, *J. Colloids and Surfaces A: Physicochemical and Engineering Aspects*, **619:** 126522 (2021).

[25] Pourakbar E., Sharifzadeh E., Synthesis of Janus/Non-Janus Hollow Graphene Oxide Micro-and Nanoparticles and the Effects of their Localization on the Thermal Conductivity of Blend-Based Polymer Composites, *J. Materials Science*, **56(32):** 18078-18092 (2021).

[26] Alam S.N., Sharma N., Kumar L., Synthesis of Graphene Oxide (GO) by Modified Hummers Method and its Thermal Reduction to Obtain Reduced Graphene Oxide (rGO), *J. Graphene*, **6(1):** 1-18 (2017).

[27] Huh S.H., Choi S.H., Ju H.M., Song C.K., Park S.H., Kim B.M, A Catalytic Graphene Oxide Film for a Dye-Sensitized Solar Cell, *J. the Korean Physical Society*, **57(6):** 1653-1656 (2010).

[28] Chen J., Yao B., Li C., Shi G., An Improved Hummers Method for Eco-Friendly Synthesis of Graphene Oxide, *J. Carbon*, **64:** 225-229 (2013).

[29] Guo H.L., Wang X.F., Qian Q.Y., Wang F.B., Xia X.H., A Green Approach to the Synthesis of Graphene Nanosheets, *J. ACS Nano*, **3(9):** 2653-2659 (2009).

[30] Malas A., Das C.K., Das A., Heinrich G., Development of Expanded Graphite Filled Natural Rubber Vulcanizates in Presence and Absence of Carbon Black: Mechanical, Thermal and Morphological Properties, *J. Materials & Design*, **39:** 410-417 (2012).

[31] Teong S.P., Li X., Zhang Y., Hydrogen Peroxide as An Oxidant in Biomass-to-Chemical Processes of Industrial Interest, *J. Green Chemistry*, **21(21):** 5753-5780 (2019).

[32] Zhu Y., Murali S., Cai W., Li X., Suk J.W., Potts J.R., Ruoff R.S., Graphene and Graphene Oxide: Synthesis, Properties, and Applications, *J. Adv. Materials*, **22(35):** 3906-3924 (2010).

[33] Shahriary L., Athawale A.A., Graphene Oxide Synthesized by using Modified Hummers Approach, *Int. J. Renew. Energy Environ. Eng*, **2(1):** 58-63 (2014).

[34] Kumar D., Singh K., Verma V., Bhatti H.S., Synthesis, Structural and Optical Characterization of Graphene Oxide and Reduced Graphene Oxide, *J. Nanoelectronics and Optoelectronics*, **9(4):** 458-467 (2014).

[35] Lai Q., Zhu S., Luo X., Zou M., Huang S., Ultraviolet-Visible Spectroscopy of Graphene Oxides, *J. Aip. Adv.*, **2(3):** 032146 (2012).